Advanced Composite Materials

ISSN: 0924-3046 (Print) 1568-5519 (Online) Journal homepage: http://www.tandfonline.com/loi/tacm20

Progressive crushing of a unidirectional CFRP plate with V-shaped trigger

Masahito Ueda, Shunsuke Anzai & Takanori Kubo

To cite this article: Masahito Ueda, Shunsuke Anzai & Takanori Kubo (2015) Progressive crushing of a unidirectional CFRP plate with V-shaped trigger, Advanced Composite Materials, 24:1, 85-95, DOI: 10.1080/09243046.2014.882540

To link to this article: http://dx.doi.org/10.1080/09243046.2014.882540

Advanced Composite Materials, 2015
Vol. 24, No. 1, 85–95, http://dx.doi.org/10.1080/09243046.2014.882540

Progressive crushing of a unidirectional CFRP plate with V-shaped trigger

Masahito Ueda*, Shunsuke Anzai and Takanori Kubo

Department of Mechanical Engineering, College of Science and Technology, Nihon University 1-8-14 Kanda-surugadai, Chiyoda, Tokyo 101-8308, Japan

(*Received 10 December 2013; accepted 9 January 2014*)

The fundamentals of progressive crushing were studied using a unidirectionally laminated carbon fiber reinforced plastic (CFRP) plate. A special test fixture was used for the test and crushing behavior of the CFRP was observed from the side. During progressive crushing, the fractured part was separated into a pillar and fronds. Fibers fractured periodically in the pillar. In contrast, fronds were delaminated without fiber fracture. The pillar carried almost all the applied load; however, the progressive crushing stress was much lower than the static compressive strength. The intervals of the periodic fiber fracture in the pillar were 50–100 μm which coincided with kink-band width of the compressive failure. Since the interval of the periodic fiber fracture varied along the pillar thickness because of the bending deformation, compressive stress also varied along the pillar thickness. The crushing stress was, therefore, much lower than the static compressive strength.

Keywords: CFRP; progressive crushing; crash energy absorption; kink-band

1. Introduction

The energy absorption capability of a well-designed carbon fiber reinforced plastic (CFRP) laminate is higher than that of metallic materials.[1–3] CFRP laminates are, therefore, being used as crash energy absorbing structures.[4–9] However, designing for energy absorption capability is not easy because it is affected by many parameters such as fiber and matrix type,[10] fiber volume fraction,[10] stacking sequence,[11–13] cross-sectional features,[14–16] and trigger geometry.[17–20]

The energy absorption capability is strongly dependent on the stacking sequence. Even when the same stacking sequence is adopted, the energy absorption capability also changes depending on the cross-sectional features. For example, in the case of hollow bar with closed section, circumferential ply constrains out-of-plane deformation which suppresses splitting of the other axial ply. The effect of the circumferential ply is, however, different dependent upon the stacking sequence and the cross-sectional features. Fracture behavior and resultant energy absorption capability of a CFRP laminate are strongly affected by a combination of the stacking sequence and the cross-sectional features. Although many progressive crushing tests of various types of CFRP laminates,

*Corresponding author. Email: ueda@mech.cst.nihon-u.ac.jp

i.e. cross-ply, angle-ply, quasi-isotropic, have been reported, the fundamentals of progressive crushing and the resultant energy absorption need to be clarified.

Open section specimens such as flat or corrugated plates have been used to study the fundamental characteristics of the energy absorption.[21–36] A unidirectional CFRP shows fundamental progressive crushing characteristics because it has the simplest stacking sequence. However, tests on these plates have not been reported, probably because splitting and delamination may result in overall failure without progressive crushing.

In this study, progressive crushing tests of a unidirectionally laminated CFRP plate were performed using a special test fixture. The test fixture was used to keep the plate parallel to the loading direction during the test. The unidirectionally laminated CFRP plate was crushed progressively without catastrophic failure and the resultant energy absorption was measured. Periodic fiber fractures due to crushing were observed microscopically to study the effect on the energy absorption. The fundamentals of progressive crushing and the resultant energy absorption capability of a unidirectional CFRP were revealed.

2. Experimental

2.1. Material and specimen configuration

A unidirectional CFRP laminate was fabricated from a prepreg sheet (PYROFIL TR30S/#380, Mitsubishi Rayon) using an autoclave molding method. The prepreg sheet was cured at 130 °C and 590 kPa pressure for 90 min, following the manufacturer's instructions. The fiber volume fraction was about 60%. A consolidated unidirectional CFRP laminate was cut into a rectangular plate, 78 mm long and 10 mm wide as shown in Figure 1(a). The stacking sequence was $[0_8]_T$ which resulted in a thickness of approximately 1.8 mm. A trigger was machined on one end of the plate to provide a weak part. The trigger would fail prior to global buckling of the plate and initiate the progressive crushing.

Many literatures about the effect of trigger geometries on progressive crushing were available. It was reported that the energy absorption capability changes with trigger geometry, even for the same CFRP.[17–20] In this study, the V-shaped trigger shown in Figure 1(b) was adopted because a unidirectional CFRP laminate progressively crushes, after which the fractured shape is symmetrical with respect to the middle of the thickness (see Figure 4). A symmetrical V-shaped trigger contributes to reproducible progressive crushing results.[37]

2.2. Test fixture for progressive crushing

A rectangular plate specimen configuration was adopted to simply assess progressive crushing of a unidirectional CFRP laminate. The test fixture for the progressive crushing test is shown in Figure 2. A specimen was placed in the test fixture with the trigger part downward. The specimen was loaded between the two out-of-plane constraining plates. The fractured CFRP was ejected freely from the test fixture to both sides. The clearance between the out-of-plane constraining plates was adjusted by shims to be 1.9 mm. No clamping force was applied to the specimen. The out-of-plane constraining plates were fixed to the base. Gage length L_g (unsupported length) was kept constant during the test, and was adjusted by shims. The chosen gage lengths were $L_g = 5$, 10 or 15 mm. The progressive crushing behavior was observed from the side

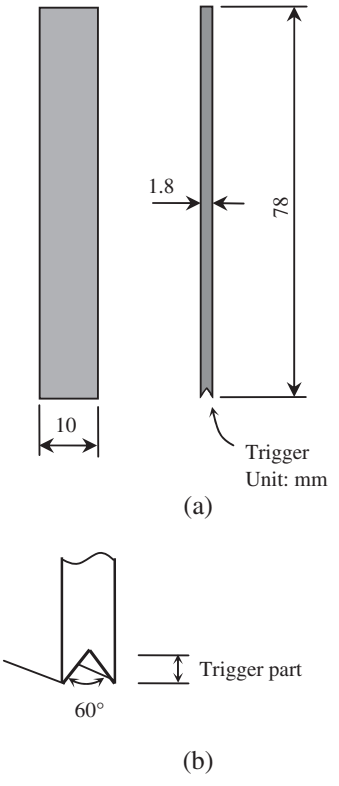

Figure 1. Specimen configuration for progressive crushing test. (a) Dimension and (b) V-shaped trigger geometry at specimen tip.

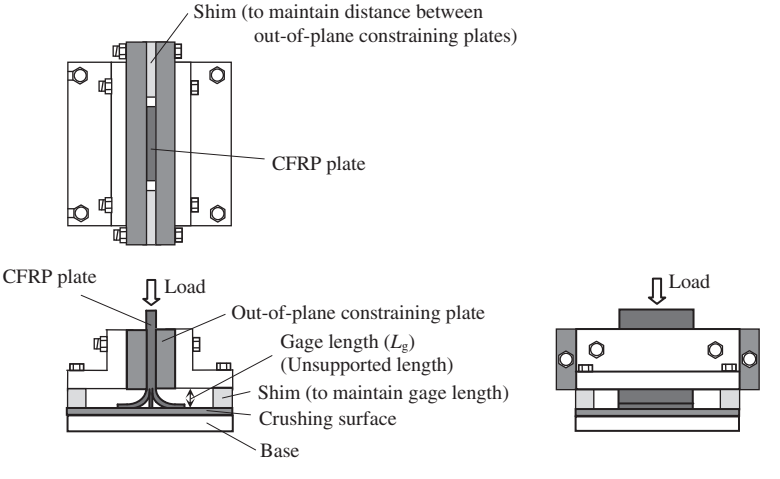

Figure 2. Test fixture for progressive crushing test.

during the test. Grease was spread onto the contact surfaces between the specimen and the test fixture to reduce the effect of friction on the progressive crushing load.

2.3. Test procedure

The progressive crushing test was performed between parallel steel platens of a universal testing machine (AG-IS, Shimadzu). The load was applied quasi-statically under displacement control with a crosshead speed of 1.0 mm/min.

2.4. Specific energy absorption

Specific energy absorption was used as an index of energy absorption capability. Specific energy absorption (Es) is defined as absorbed energy per unit mass.

$$Es = \frac{1}{M}\int_0^{L_e} P\,dL = \frac{P_a L_e}{M} \quad [\mathrm{kJ/kg}] \tag{1}$$

where P is the progressive crushing load, L_e is the crushed length of a specimen, M is the mass of a specimen, and P_a is the average progressive crushing load. Here, it is usually assumed that $L_e = L_t$ (specimen length) because of the characteristics of progressive crushing of a CFRP laminate.[11] Then, Equation (1) is rewritten as:

$$Es = \frac{\sigma_a}{\rho} \quad [\mathrm{kJ/kg}] \tag{2}$$

where σ_a is the average progressive crushing stress and ρ is the density of a specimen (=1.5 g/cm^3).

3. Results and discussion

3.1. Observation of progressive crushing

Progressive crushing tests of a unidirectionally laminated CFRP plate with a V-shaped trigger were performed at various gage lengths, $L_g = 5$, 10 or 15 mm. Load-displacement curves are shown in Figure 3. Figure 4 shows side view pictures during progressive crushing when $L_g = 15$ mm. The numbers (i)–(iv) in Figure 3 correspond to those in Figure 4.

In region (i), the load increased with increasing displacement. Local failure was initiated at the tip of the trigger. The maximum load was recorded at point (ii). Immediately after that, the load decreased suddenly with onset of delamination. In region (iii), the load has been decreased by onset and propagation of delamination. Intermittent initiation and propagation of delamination were observed. A column-like 'pillar' was observed around the middle of the thickness. The surface layers were delaminated and bent at both sides of the pillar; these bent layers are generally called 'fronds'.[11] In the fronds, fiber bridging was observed at the delaminated area. In region (iv), the load remained almost constant with stable progressive crushing in which the pillar thickness and curvature of the fronds remained almost constant. Therefore, the progressive crushing was transient in regions (i)–(iii), and stable in region (iv). It should be noted that the delamination length was less than the gage length in this case ($L_g = 15$ mm). Out-of-plane constraining plates did not directly suppress delamination.

Figure 5 shows load-displacement curves of five specimens with $L_g = 10$ mm. Progressive crushing load in the region (iv) varied slightly between specimens. The trigger geometry affects the initial fracture behavior, which also affects the ensuing crushing mode. The progressive crushing load, therefore, varied because of variations in the machining of the V-shaped trigger. Fiber bridging in the fronds indicates fiber

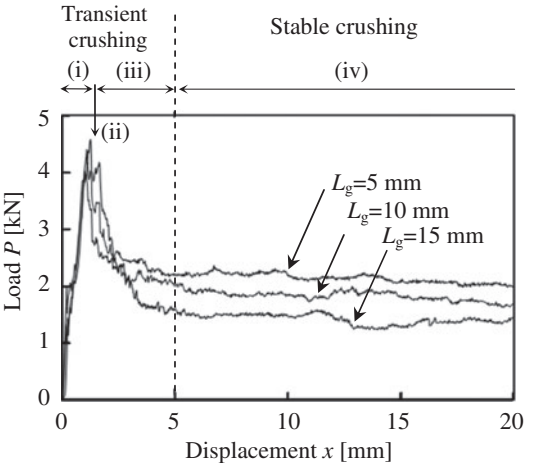

Figure 3. Load-displacement curves for unidirectionally laminated CFRP plate with V-shaped trigger (gage lengths $L_g = 5$, 10, and 15 mm).

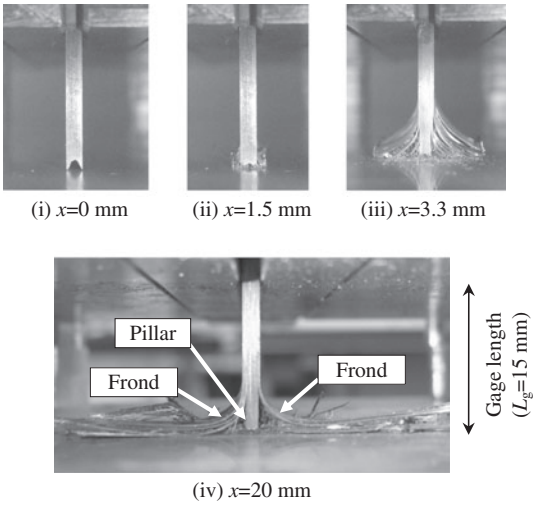

Figure 4. Successive pictures of progressive crushing ($L_g = 15$ mm).

waviness in the unidirectional CFRP laminate. The boundary between the pillar and fronds may shift as a result of local fiber waviness. The progressive crushing load, therefore, also varied due to the fiber waviness.

Progressive crushing load in the stable region (iv) tended to increase with decreasing gage length. Delamination length was less than or almost equal to L_g when $L_g = 10$ mm, as shown in Figure 6(a) or (b). In contrast, delamination length was always equal to gage length when $L_g = 5$ mm, as shown in Figure 6(c). If the delamination length is equal to the gage length, the out-of-plane constraining plates directly suppress delamination, which increases the pillar thickness. The effect of constraining on pillar thickness is discussed in the following section.

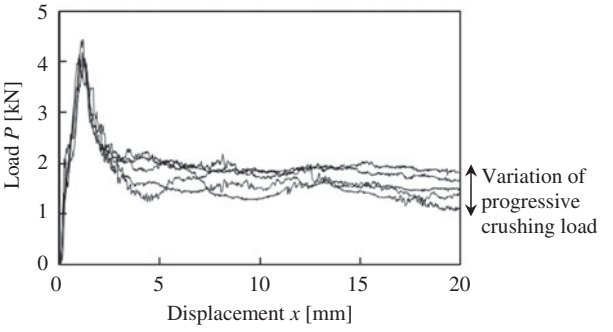

Figure 5. Variation of progressive crushing load ($L_g = 10$ mm).

3.2. *Progressive crushing stress and specific energy absorption*

Progressive crushing load was almost constant during stable progressive crushing (iv), although it varied somewhat between specimens of the same gage length. The pillar thickness also varied between specimens. The effect of the pillar thickness on the progressive crushing load, i.e. the energy absorption capability, was investigated.

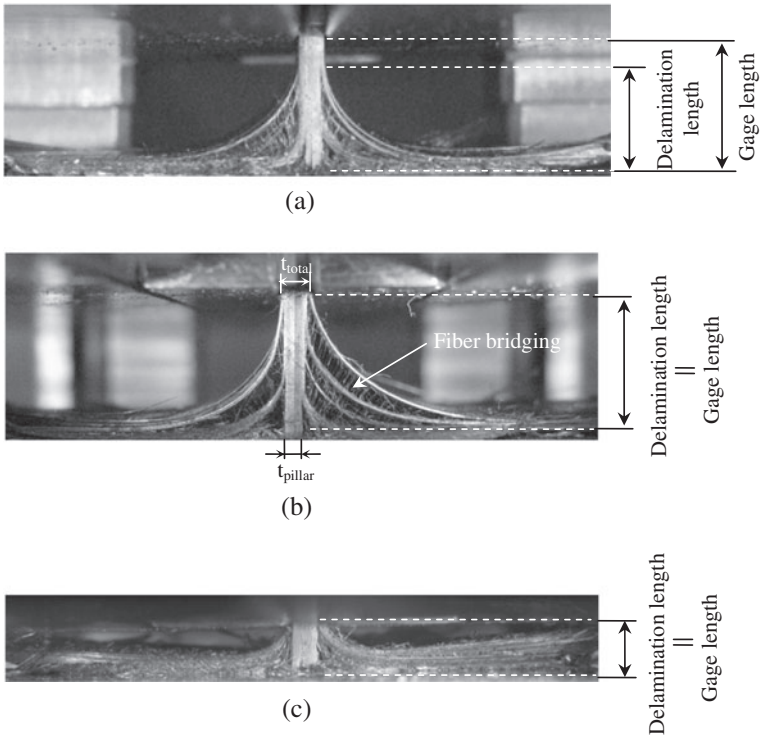

Figure 6. Relation between gage length and delamination length. (a) $L_g = 10$ mm (Delamination length < gage length), (b) $L_g = 10$ mm (Delamination length = gage length), and (c) $L_g = 5$ mm (Delamination length = gage length).

Figure 7 shows the progressive crushing stress as a function of pillar thickness. The abscissa is the ratio of pillar thickness t_{pillar} to total specimen thickness t_{total}. The pillar thickness was taken as the average of the values measured on both sides of the specimen. The left ordinate is the progressive crushing stress, calculated from the progressive crushing load divided by the cross-sectional area. Here, the progressive crushing load and the pillar thickness were measured when the displacement was 20 mm i.e. $P_{x=20\,mm}$ was substituted to P_a. The right ordinate is the instantaneous value of specific energy absorption.

The progressive crushing stress is almost linearly proportional to the pillar thickness. This result indicates that the pillar is a dominant factor in the energy absorption. However, the progressive crushing stress was relatively higher than the linear curve shown in Figure 7 when $L_g = 5$ mm. The curvature radius of fronds became small when $L_g = 5$ mm, which prevented the progress of displacement and apparently increased the progressive crushing stress. The maximum progressive crushing stress was about 150 MPa; this was calculated by linear extrapolation in Figure 7 assuming that the total cross-sectional area was pillar. This may be considered as a static compressive strength of the unidirectional CFRP laminate, although this extrapolated maximum progressive crushing stress is only 15% of the static compressive strength. The static compressive strength was about 996 MPa followed by ASTM D695. The progressive crushing stress in region (iv) is much lower than the static compressive strength.

3.3. *Microscopic observation of pillar*

After the progressive crushing test, the specimen was taken from the test fixture. It was cut along the middle of its width, and is shown in Figure 8. Fronds sprang back almost to their original positions. Fracture in the fronds is mostly delamination. In contrast, the shape of the pillar remained deformed, and some parts were missing parts because of the severe damage. Fracture in the pillar is mostly fiber fracture. The fracture modes differ greatly between the frond and the pillar.

When the specimen was taken from the test fixture after the progressive crushing test, the pillar was forced to deform by the spring back of the fronds. Therefore, another specimen was filled with epoxy resin (105/206, West system) while still in the test fixture, before unloading, so that the fracture could be observed without further

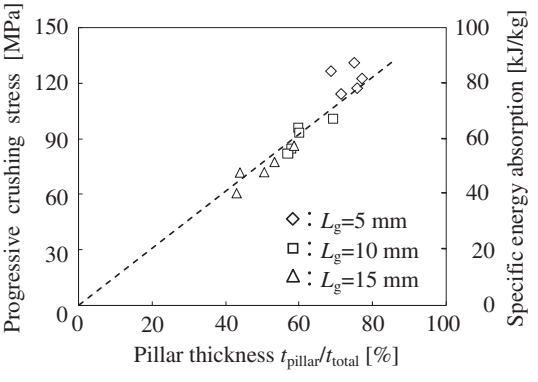

Figure 7. Progressive crushing stress as a function of pillar thickness.

Figure 8. A unidirectionally laminated CFRP plate taken from the test fixture after progressive crushing test ($L_g = 15$ mm).

deformation. After the resin was completely cured, the specimen was unloaded and taken from the test fixture. The specimen was then cut along the middle of the width. The pillar region was observed using an optical microscope and scanning electron microscope (SEM); images are shown in Figure 9. Before optical microscopy, the surface was carefully polished using an abrasive compound. Prior to SEM, a small amount of the matrix on the surface was slightly removed using sulfuric acid to observe the fiber fracture.

A large crack is observed at the middle of the pillar, where the pillar has been split into two parts, both of which were bent in opposite directions with small radius of curvature. Periodic fiber fracture is observed throughout the pillar, with the interval of the periodic fiber fracture being shorter at the outside of the pillar than at the inside.

Figure 10(a) and (b) shows periodic fiber fracture observed at the outer side of the pillar of samples tested at $L_g = 5$ and 10 mm, respectively. The intervals of the periodic fiber fracture are approximately 50 μm. There was no clear difference with gage length. This interval almost coincides with kink-band length of the compressive failure.[38–40] Since the interval of the periodic fiber fracture varies along the pillar thickness because of the bending deformation, compressive stress also varies along the pillar thickness. The extrapolated maximum progressive crushing stress in Section 3.2 estimated a stress that was less than the static compressive strength.

4. Conclusions

Progressive crushing tests of a unidirectionally laminated CFRP plate with V-shaped trigger were performed using a special test fixture. The fundamentals of progressive crushing behavior and resultant energy absorption were revealed. The main results obtained in this paper were:

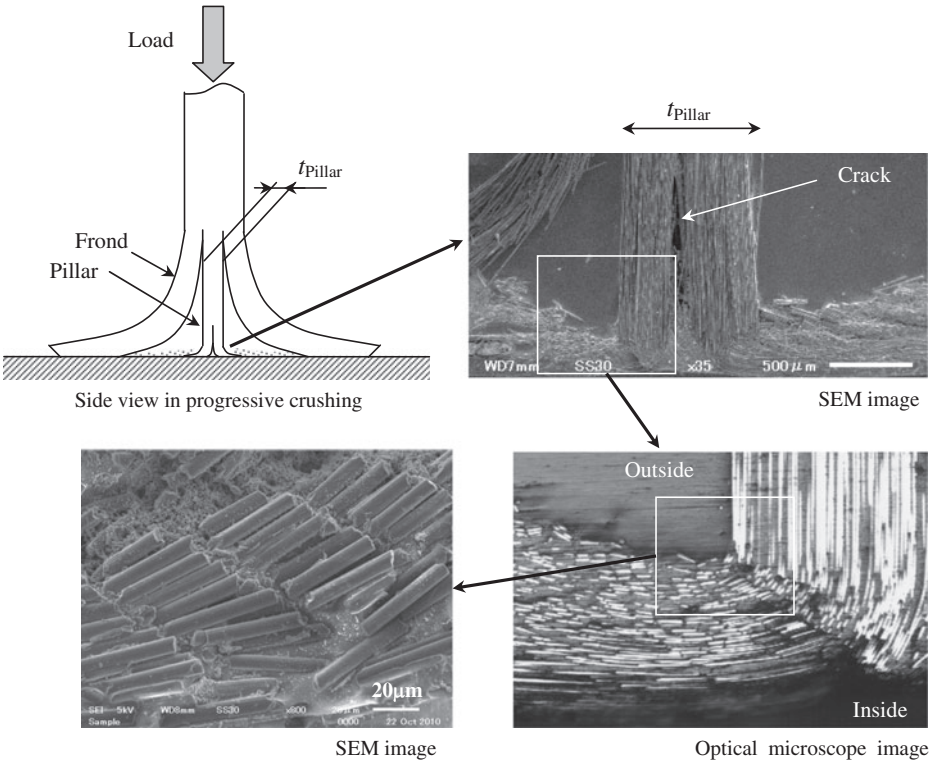

Figure 9. Cross-sectional observations of pillar after progressive crushing.

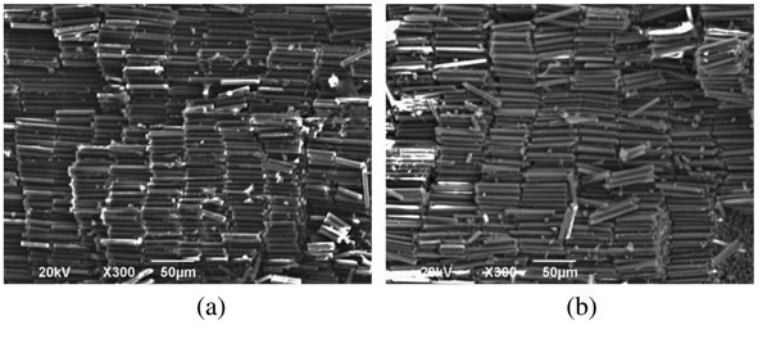

Figure 10. Periodic fiber fracture at outside of pillar. (a) $L_g = 5$ mm and (b) $L_g = 10$ mm.

(1) The fractured part was separated into a pillar and fronds during progressive crushing. Fibers in the pillar fractured periodically. The fronds were delaminated without fiber fracture. The fracture mode differed greatly between the pillar and the fronds.
(2) Progressive crushing stress and the resultant specific energy absorption almost linearly increased with increase of pillar thickness. The progressive crushing

stress was, however, much lower than the static compressive strength, although maximum progressive crushing stress was estimated by assuming that the total thickness was a pillar.

(3) The intervals of periodic fiber fracture at the outer side of the pillar were almost same as the fiber kink-band width in the static compressive failure. The intervals varied along the pillar thickness because of the bending deformation, which resulted in lower crushing stress than the static compressive strength.

References

[1] Thornton PH, Jeryan R. Crash energy management in composite automotive structures. Int. J. Impact Eng. 1988;7:167–180.
[2] Mamalis AG, Robinson M, Manolakos DE, Demosthenous GA, Ioannidis M, Carruthers J. Crashworthy capability of composite material structures. Compos. Struct. 1997;37:109–134.
[3] Jacob GC, Fellers JF. Energy absorption in polymer composite materials for automotive crashworthiness. J. Compos. Mater. 2002;36:813–850.
[4] Sen JK. Designing for a crashworthy all-composite helicopter fuselage. J. Am. Helicopter Soc. 1987;32:56–66.
[5] Farley GL. Crash energy absorbing subfloor beam structure. J. Am. Helicopter Soc. 1987;32:28–38.
[6] Jackson KE, Lyle KH. Full-scale crash test and finite element simulation of a composite prototype helicopter. NASA/TP-2003-212641.
[7] Mercedes-Benz SLR McLaren. Technology for the 21st-century. Auto Technol. 2003;5: 28–31.
[8] Bisagni C, Di Pietro G. Progressive crushing of fiber-reinforced composite structural components of a Formula One racing car. Compos. Struct. 2005;68:491–503.
[9] Kawamura N. The light weight body structure technologies of Lexus LFA. In: Proceedings of 12th Japan International SAMPE Symposium; 2011 Nov 9–11; Tokyo, Japan.
[10] Farley GL. The role of fiber and matrix in crash energy absorption of composite materials. J. Am. Helicopter Soc. 1989;34:52–58.
[11] Hull D. A unified approach to progressive crushing of fibre-reinforced composite tubes. Compos. Sci. Technol. 1991;40:377–421.
[12] Hamada H, Ramakrishna S, Sato H. Effect of fiber orientation on the energy absorption capability of carbon fiber/PEEK composite tubes. J. Compos. Mater. 1996;30:947–963.
[13] Ochelski S, Gotowicki P. Experimental assessment of energy absorption capability of carbon-epoxy and glass-epoxy composites. Compos. Struct. 2008;87:215–224.
[14] Farley GL. Effect of specimen geometry on the energy absorption capability of composite materials. J. Compos. Mater. 1986;20:390–400.
[15] Mamalis AG, Yuan YB, Viegelahn. Collapse of thin-wall composite sections subjected to high speed axial loading. Int. J. Veh. Des. 1992;13:564–579.
[16] Hamada H, Ramakrishna S. Scaling effects in the energy absorption of carbon-fiber/PEEK composite tubes. Compos. Sci. Technol. 1995;55:211–221.
[17] Czaplicki MJ, Robertson RE, Thornton PH. Comparison of bevel and tulip triggered pultruded tubes for energy absorption. Compos. Sci. Technol. 1991;40:31–46.
[18] Sigalas I, Kumosa M, Hull D. Trigger mechanisms in energy-absorbing glass cloth/epoxy tubes. Compos. Sci. Technol. 1991;40:265–287.
[19] Thuis HGSJ, Metz VH. The influence of trigger configurations and laminate lay-up on the failure mode of composite crush cylinders. Compos. Struct. 1993;25:37–43.
[20] Jiménez MA, Miravete A, Larrodé E, Revuelta D. Effect of trigger geometry on energy absorption in composite profiles. Compos. Struct. 2000;48:107–111.
[21] Lavoie JA, Morton J. A crush test fixture for investigating energy absorption of flat composite plates. Exp. Tech. 1994;18:23–26.
[22] Jackson K, Morton J, Lavoie JA, Boitnott R. Scaling of energy absorbing composite plates. J. Am. Helicopter Soc. 1994;39:17–23.

[23] Fleming DC, Vizzini AJ. Off-axis energy absorption characterization of composites for crashworthy rotorcraft design. J. Am. Helicopter Soc. 1996;41:239–249.
[24] Lavoie JA, kellas S. Dynamic crush tests of energy-absorbing laminated composite plate. Compos. Part A. 1996;27:467–475.
[25] Fleming DC, Vizzini AJ. The energy absorption of composite plates under off-axis loads. J. Compos. Mater. 1996;30:1977–1995.
[26] Dubey DD, Vizzini AJ. Energy absorption of composite plates and tubes. J. Compos. Mater. 1998;32:158–176.
[27] Dubey DD, Vizzini AJ. Testing methods for energy absorption of kevlar/epoxy. J. Am. Helicopter Soc. 1999;44:179–187.
[28] Daniel L, Hogg PJ, Curtis PT. The relative effects of through-thickness properties and fibre orientation on energy absorption by continuous fibre composites. Compos. Part B. 1999;30:257–266.
[29] Daniel L, Hogg PJ, Curtis PT. The crush behavior of carbon fibre angle-ply reinforcement and the effect of interlaminar shear strength on energy absorption capability. Compos. Part B. 2000;31:435–440.
[30] Jacob GC, Starbuck JM, Simunovic S, Fellers JF. New test method for determining energy absorption mechanisms in polymer composite plates. Polym. Compos. 2003;24:706–715.
[31] Fleming DC, Nicot F. Crushing of flat graphite/epoxy laminates using a column specimen. J. Compos. Mater. 2003;37:2225–2239.
[32] Savona SC, Hogg PJ. Investigation of plate geometry on the crushing of flat composite plates. Compos. Sci. Technol. 2006;66:1639–1650.
[33] Cauchi Savona S, Hogg PJ. Effect of fracture toughness properties on the crushing of flat composite plates. Compos. Sci. Technol. 2006;66:2317–2328.
[34] Feraboli P, Deleo F, Garattoni F. Efforts in the standardization of composite materials crashworthiness energy absorption. In: Proceedings of 22nd ASC Technical Conference; Seattle, Washington; 2007.
[35] Feraboli P. Development of a corrugated test specimen for composite materials energy absorption. J. Compos. Mater. 2008;42:229–256.
[36] Feraboli P, Wade B, Deleo F, Rassaian M. Crush energy absorption of composite channel section specimens. Compos. Part A 2009;40:1248–1256.
[37] Ueda M, Takashima T, Kato Y, Nishimura T. Progressive crushing behavior and energy absorption of unidirectional CFRP plate under axial compression. J. Jpn Soc. Compos. Mater. 2010;36:104–111.
[38] Budiansky B. Micromechanics. Comput. Struct. 1983;16:3–12.
[39] Jumahat A, Soutis C, Jones FR, Hodzic A. Fracture mechanisms and failure analysis of carbon fibre/toughened epoxy composites subjected to compressive loading. Compos. Struct. 2010;92:295–305.
[40] Gutkin R, Pinho ST, Robinson P, Curtis PT. On the transition from shear-driven fibre compressive failure to fibre kinking in notched CFRP laminates under longitudinal compression. Compos. Sci. Technol. 2010;70:1223–1231.